Surface oxidation of the icosahedral Ag-In-Yb quasicrystal

P. J. Nugent,[1] G. Simutis,[1] V. R. Dhanak,[1] R. McGrath,[1] M. Shimoda,[2] C. Cui,[3] A. P. Tsai,[2,3] and H. R. Sharma[1]
[1]*Surface Science Research Centre and Department of Physics, The University of Liverpool, Liverpool L69 3BX, United Kingdom*
[2]*National Institute for Materials Science, 1-2-1 Sengen, Tsukuba, Ibaraki 305-0047, Japan*
[3]*Institute of Multidisciplinary Research for Advanced Materials, Tohoku University, Sendai 980-8577, Japan*
(Received 13 April 2010; revised manuscript received 20 May 2010; published 9 July 2010)

The oxidation of the high-symmetry surfaces of a single grain icosahedral (*i*) Ag-In-Yb quasicrystal has been studied using x-ray photoemission spectroscopy. The oxidation was carried out in vacuum, air, and water. It is found that air exposure results in the same degree of oxidation as exposure to oxygen in vacuum. The oxidation in water is more effective. Among the three constituent elements, the core levels of Yb are most affected by oxidation, Ag core levels are unchanged, and In shows moderate effects as expected from heats of formation of bulk oxides of the three elements. The comparison of the results with pure elements also reveals that the oxidation of Ag, In, and Yb in the quasicrystal is very similar to that of pure elements in all three environments. Scanning tunneling microscopy and low-energy electron diffraction reveal that oxidation destroys the quasicrystalline order of the clean surface.

DOI: 10.1103/PhysRevB.82.014201 PACS number(s): 71.23.Ft, 79.60.−i, 68.43.−h

I. INTRODUCTION

Since their discovery quasicrystals have attracted much attention because of their aperiodic long-range order with forbidden rotational symmetries.[1] It is of great interest to understand how the aperiodic order influences the physical properties and characteristics of a material. The unusual tribological and transport properties of quasicrystals[2] such as low coefficient of friction and high electrical and thermal resistivity, which are important for technological applications, are found to be affected by the surface oxide layer formed due to ambient atmosphere.[3,4] Hence it is crucial to understand the oxidation process in order to explain the variations in these properties. Several studies have been carried out on the oxidation of Al-based quasicrystals.[5–7] However, up to now there have been no reports concerning the oxidation behavior of *i*-Ag-In-Yb, which belongs to the *i*-Cd-Yb family of quasicrystals.

The discovery of the binary *i*-Cd-Yb quasicrystal[8] was a major advance in the field as its structure could be fully determined using x-ray diffraction.[9] Moreover, theoretical and experimental work on this phase has provided insight on the stability of icosahedral quasicrystals[10,11] and on the origin of their transport properties.[12–14] The *i*-Cd-Yb phase is unsuitable for studies in ultrahigh vacuum (UHV) due to the high vapor pressure of Cd which evaporates upon heat treatments. However, it is possible to grow a quasicrystal with the same structure as *i*-Cd-Yb by replacing Cd by other elements such that the valence electron to atom ratio remains the same as that of *i*-Cd-Yb,[15] i.e., $e/a=2.0$. One such quasicrystal is *i*-Ag-In-Yb, which is the subject of this study.

The first UHV surface study of *i*-Ag-In-Yb (Ref. 16) was followed by a structure determination of the fivefold surface using scanning tunneling microscopy (STM) and the bulk model of *i*-Cd-Yb,[17] which showed that the surface termination is characteristic of bulk truncation.[17] The study of this material with a wider range of surface science techniques was hampered by the limited size of the available samples.[18] However, recent success in the growth of large, high-quality samples has permitted the employment of such techniques, for example, ultraviolet photoemission spectroscopy (UPS).[19] UPS results combined with electronic-structure calculations have revealed that the valence band of *i*-Ag-In-Yb near to the Fermi level is dominated by the Yb 4*f*-derived states. The calculation reveals that the pseudogap in the density of states is due to a hybridization of the Yb 5*d* band with the Ag 5*p* and In 5*p* bands (*p*-*d* hybridization),[19] as in the case of *i*-Cd-Yb.[11] Originally, it was thought that the pseudogap of an icosahedral quasicrystal is due to the Hume-Rothery mechanism combined with *sp*-*d* hybridization.[20] The valence band of *i*-Ag-In-Yb shows features similar to those of pure Yb.[19]

The aim of this work is to analyze the core-level electronic structure of *i*-Ag-In-Yb and to study the surface oxidation process in three different environments: vacuum, air, and water and compare the oxidation behavior with that of the pure elements Ag, In, and Yb in similar conditions, using x-ray photoemission spectroscopy (XPS). We also employed STM and low-energy electron diffraction (LEED) to investigate surface ordering after oxidation. The oxidation was carried out on three high-symmetry surfaces: fivefold, threefold, and twofold.

II. EXPERIMENTAL DETAILS

An ingot of a single grain *i*-$Ag_{42}In_{42}Yb_{16}$ grown by the Bridgman method[15] was cut perpendicular to the fivefold (5f), threefold (3f), and twofold (2f) axes. Each sample was then mechanically polished with successively finer grades of diamond paste down to 0.25 μm prior to introduction into the UHV chamber. In UHV the samples were degassed for about 12 h at a temperature of about 350 °C while keeping the pressure to 1×10^{-9} mbar or lower. The samples were then cleaned by several cycles of Ar^+ sputtering (2 keV, 30 min) and annealing (420–440 °C, 2 h). The surface composition and cleanness were monitored by XPS with unmonocromatized Al K_α radiation ($h\nu=1486.6$ eV) using a PSP Vacuum Technology hemispherical electron-energy ana-

lyzer. It was generally found that after this initial conditioning of the samples, subsequent cleaning by sputtering for 15 min followed by annealing for an hour was sufficient to produce clean surfaces with composition similar to the bulk as determined by XPS.

For studies of pure elements, 99.9% pure In and Yb foils and a Ag(111) single crystal were used. Each sample was cleaned by Ar^+ sputtering and as in the case of the quasicrystal samples XPS was used to assess the cleanness. The Yb sample was difficult to prepare: a trace of oxygen was detectable by XPS even after many cycles of sputtering. These reference samples were used to calibrate the XPS core-level binding energies (BEs) while oxygen adsorption on these surfaces was useful in identifying oxidation states on the quasicrystal surfaces.

Oxidation in vacuum was carried out by introducing 99.6% pure oxygen gas through a leak valve into the UHV chamber at different exposures ranging from sub-Langmuir (L) to 10^3 L or higher. Oxygen pressure was 1×10^{-8} mbar for exposures <10 L, 5×10^{-7} mbar for 10–100 L, and 1×10^{-6} mbar for higher exposures. For air oxidation of the quasicrystals, the samples were exposed to the atmosphere in the fast entry load-lock chamber for 15 h. The samples were cleaned before the exposure to air. The Yb and In foils were exposed to the atmosphere for longer than 15 h. For oxidation in water, the samples were dipped into distilled water. The water exposure time was 24 h for the quasicrystals and the Yb foil and 15 h for the In foil. Prior to water exposure, the quasicrystals were sputter annealed in UHV but they were briefly exposed to the atmosphere while transferring to water.

All XPS measurements and oxygen exposures were performed at room temperature. XPS measurements were made at an angle of 15° to the normal emission, except for polar angle-dependent measurements for which angle is varied from 15° to 75°.

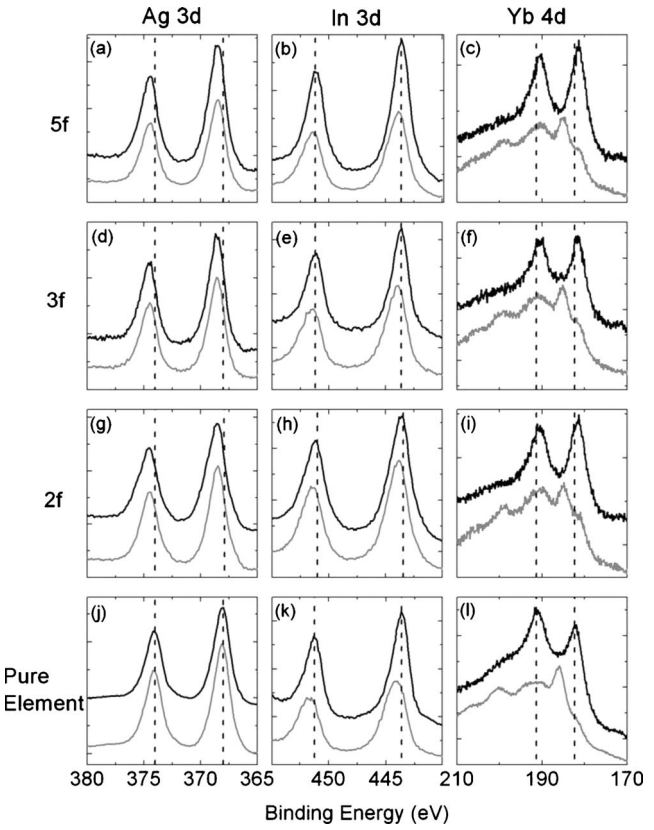

FIG. 1. XPS Ag 3*d* (first column), In 3*d* (second column), and Yb 4*d* (third column) spectra from the clean [(a)–(c)] fivefold, [(d)–(f)] threefold, and [(g)–(i)] twofold *i*-Ag-In-Yb surfaces and (j) Ag(111), (k) pure In, and (l) Yb foils (black curves) and the corresponding spectra after oxidation in vacuum (gray curve). Oxygen exposure was 1000 L for all surfaces except for the Yb foil which was exposed to 10 L. The vertical dotted line marks the peak position for pure elements. Spectra were taken with 50 eV pass energy of the analyzer.

III. RESULTS AND DISCUSSION

A. Characterization of clean surfaces

The structure of the fivefold,[17] threefold,[21] and twofold[21] surfaces of *i*-Ag-In-Yb were characterized by STM and LEED. LEED pattern from the fivefold surface after annealing reveal quasicrystalline long-range order with the symmetry expected from the bulk. The surfaces exhibit large terraces in STM. The comparison of the STM results with the bulk structure of the isostructural *i*-Cd-Yb suggests that the surfaces are formed at bulk positions which are dense and intersect the center of rhombic triacontahedral clusters,[9] the building blocks of the system. The topmost surface layer in the fivefold surface, for example, is composed of up to 50% Yb. The exact distribution of In and Ag atoms is not yet known. However, based on the structure of the Ag-In-Yb approximant,[22] it can be inferred that the topmost layer of the fivefold surface contains more In than Ag. This is reflected in oxidation studies (Sec. III B).

The change in surface composition upon sputtering and annealing was previously analyzed for the fivefold surface.[16] It was found that the sputtering preferentially removes In and Yb resulting in Ag enrichment in the surface region. Annealing restores a surface composition close to the bulk. We reanalyze the surface composition because the samples used in the current study were grown under different conditions than the previous samples and showed different structural qualities.[18] The previous samples,[23] which were grown at a slower rate,[15] exhibited different domains and impurity phases.[18] In contrast, the current samples are structurally perfect and the structure is uniform all over the sample. We determine that the composition of all three (fivefold, threefold, and twofold) surfaces, which ranges between 62–63 % Ag, 27–28 % In, and 9–10 % Yb after sputtering, is consistent with the previous results.[16] The composition after annealing is 35–38 % Ag, 43–45 % In, and 19–20 % Yb, which is close to the bulk composition. We note that these values refer to the compositions of several surface layers.

Figures 1(a)–1(i) shows the Ag 3*d*, In 3*d*, and Yb 4*d* core levels for the fivefold, threefold, and twofold surfaces after annealing. Spectra for the pure In and Yb foils and Ag(111) are given in Figs. 1(j)–1(l) for comparison. The corresponding spectra for the quasicrystal samples and for the pure elements after in-vacuum oxidation are also presented. These

TABLE I. BE and FWHM of the core-level peaks for pure elements and the fivefold, threefold, and twofold *i*-Ag-In-Yb surfaces after annealing (upper panel) and the respective values after oxidation in vacuum (lower panel). The values are in the units of electron volt with uncertainty of ±(0.1–0.2) eV. The FWHM were determined from spectra taken with 10 eV pass energy. FWHM of the Yb peaks are not given because of complex nature of the spectra after oxidation (see text).

	Ag $3d_{5/2}$		In $3d_{5/2}$		
	BE	FWHM	BE	FWHM	Yb 4*d*
Pure element	368.1	1.0	443.6	1.1	182.3, 191.3
5f	368.5	1.1	443.6	1.1	181.5, 190.6
3f	368.5	1.1	443.6	1.2	181.7, 190.6
2f	368.6	1.2	443.5	1.2	181.6, 190.6
			After oxidation		
Pure element	368.1	1.0	444.0	1.5	
5f	368.5	1.1	443.9	1.4	181.6, 185.0
					189.5, 199.0
3f	368.6	1.1	443.9	1.7	
2f	368.6	1.2	443.9	1.5	

spectra will be discussed in Sec. III B. The full width at half maxima (FWHM) and positions of the core-level peaks for each clean and oxidized sample are given in Table I. These values were determined by fitting the XPS spectra using the CASA XPS program.[24] The peaks were fitted with a combination of a Gaussian and a Lorentzian function.[25,26] A combination of 60% Gaussian and 40% Lorentzian contributions provided the best fit. The background is considered to be linear. We used the same method of fitting for other spectra discussed in this report. The uncertainty in peak positions is ±(0.1–0.2) eV. For the analysis of peak intensity, which will be discussed in Sec. III B, we recorded the area of the measured peaks (not of the fits) after a linear background subtraction.

The binding energies for Ag and Yb in the quasicrystal are different from those of the pure elements. For instance, the Ag 3*d* peaks are shifted to higher binding energies by about 0.5 eV while the Yb 4*d* peaks are shifted by about 0.7 eV to lower binding energies. However, the binding energies for In in the quasicrystal are same as for pure In. This suggests that charge is transferred from Ag to Yb in the alloy. The observed line shape of Yb 4*d* in the quasicrystal is characteristic of divalent Yb as observed in other Yb compounds[27] and as expected for this class of quasicrystal.[11]

The XPS spectra for all three quasicrystal surfaces after annealing are identical in position and width. This may not be so surprising because with the selected experimental parameters, especially the angle of detection, XPS detects several surface layers. This combined with the relatively low-energy resolution of the system means that any differences in the top layers if there are any will hardly be detected. This is evidenced by the XPS spectra from the surfaces after sputtering. As mentioned earlier sputtering depletes Yb and In in the surface region. However, the core-level spectra from the sputtered surfaces were found to be identical to those obtained after annealing. In contrast, the valence-band spectra were affected by sputtering, as discussed in Ref. 19.

B. Oxidation in vacuum

Oxidation in vacuum was carried out on all three *i*-Ag-In-Yb surfaces (after annealing) at different exposures successively up to 10^3 L. The evolution of the Ag 3*d*, In 3*d*, Yb 4*d*, and O 1*s* spectra from the fivefold surface with oxygen exposure is given in Figs. 2(a)–2(d). The spectra from the In and Yb foils after oxygen exposure are presented in Figs. 2(e) and 2(f). After oxygen exposure, the In 3*d* peaks are shifted to higher binding energies and their FWHM increases and the Yb 4*d* spectra develop new features at higher binding energies, while the Ag peaks remain unchanged in position and width. The increase in the FWHM, the peak

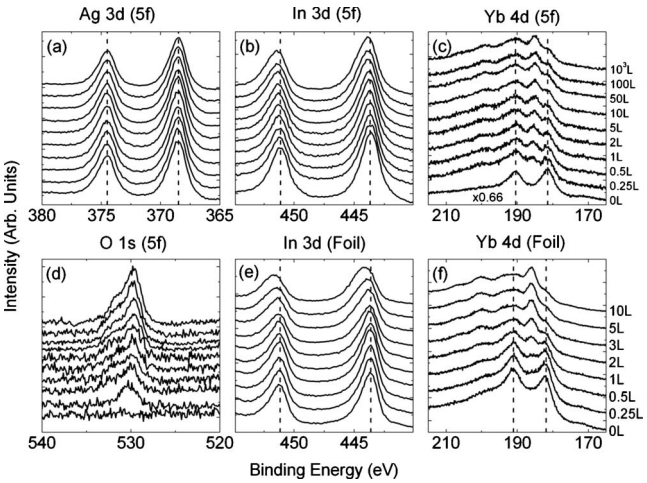

FIG. 2. XPS spectra from the fivefold *i*-Ag-In-Yb surface [(a)–(d)] and In (e) and Yb (f) foils with increasing exposures (bottom to top). The exposure was from 0.25 ML to 10^3 L for all samples except Yb foil which was exposed from 0.25 ML to 10 L.

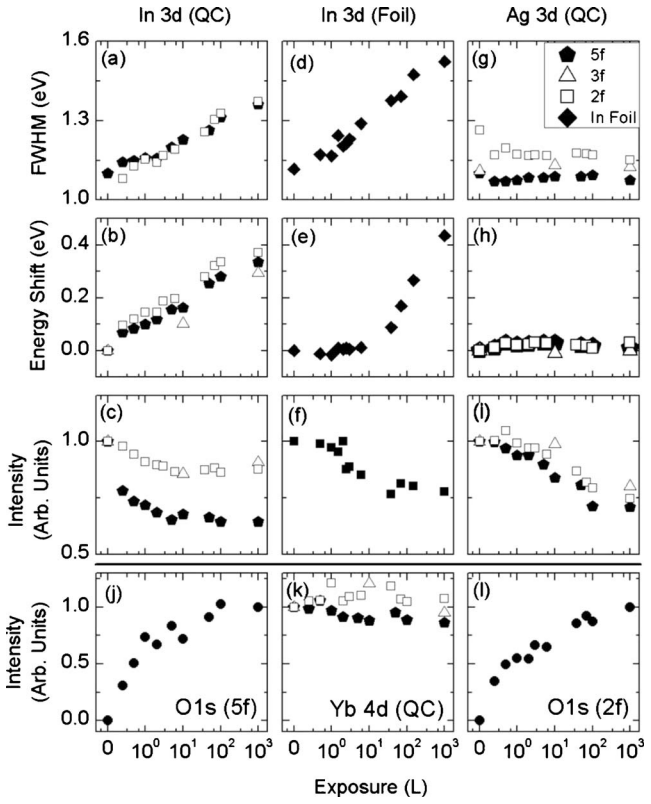

FIG. 3. Change in the FWHM, position, and intensity of core-level peaks as a function of oxygen exposure for the fivefold, threefold, and twofold *i*-Ag-In-Yb surfaces and pure elements. [(a)–(c)] In 3*d* for quasicrystal surfaces, [(d)–(f)] In 3*d* for In foil, and [(g)–(i)] Ag 3*d* for quasicrystal surfaces. [(j) and (l)] O 1*s* intensity for the fivefold and twofold surfaces. (k) Yb 4*d* intensity for quasicrystal surfaces. The intensity of the In 3*d*, Ag 3*d*, and Yb 4*d* peaks is normalized with respect to the value for the clean surface (0 L exposure) whereas the intensity of the O 1*s* peak is normalized by the value obtained after 10^3 L exposure.

shift and the modification in the core levels manifest the oxidation of In and Yb. We note that the binding-energy shift in XPS contains contributions from both initial- and final-state effects.[28] Initial-state effects originate from the local Madelung potential and the ground-state valence levels, reflecting the ground-state chemistry. On the other hand, final-state effects arise from the charge redistribution or relaxation of the core hole following the photoemission process. In XPS analysis of oxides, the final-state and Madelung potential contributions to the binding energies are often neglected and it is assumed that the shift predominantly reflects the initial-state chemistry. In our measurements, it is not possible to separate the initial- and final-state contributions to the shift in binding energies, but consider the shift to be dominated by initial-state effects which is not unreasonable.

The results of quantitative analysis of oxidation in terms of FWHM, peak shift, and intensity are presented in Fig. 3. Because of the complex nature of the peaks after oxidation, it is difficult to reliably analyze the FWHM and peak shift for Yb 4*d*. The Yb 4*d* levels are influenced at exposures less than 1 L. At these exposures, the spin-orbit doublets of the clean surface at 181.5 and 190.6 eV are accompanied by oxide peaks at around 185 and 199 eV [Fig. 2(c)]. The intensity of these peaks increases with oxygen exposure. A trace of the metallic peaks is still detectable even after 10^3 L exposure. From previous studies on oxidation of Yb thin film produced by evaporation,[29] we expect to observe five peaks related to the oxide states, in addition to the two metallic peaks in the given range of binding energies. With the resolution of our system, it is not possible to resolve all of these features and thus to quantify the metallic and oxide contribution. This creates difficulties in determining the thickness of oxide layer using the intensity of oxide and metallic peaks, in contrast to the Al-based alloys where metallic and oxide peaks for the Al 2*p* level are clearly separated.[30] The estimation of the oxide thickness is, however, possible from polar angle-dependent XPS measurements, which will be discussed later in this section. For the Yb peak, the total intensity due to metallic and oxide contributions is almost invariant for all exposures, indicating that there is no segregation of Yb on to the surface, unlike in the Al-based quasicrystals where oxidation induces segregation of Al to the surface which forms a passivating aluminum oxide layer.[5,6]

The oxidation behavior of Yb in the quasicrystal is very similar to that of pure Yb. As shown in Fig. 2(f), pure Yb also oxidizes at very low exposure yielding additional peaks at higher binding energies. The separation of these peaks from the metallic peaks is the same as in the quasicrystal. High exposure produces a complex structure with a remnant of metallic peaks as in the quasicrystal.

Figures 3(a)–3(c) shows the variation in the FWHM, position, and intensity of the In $3d_{5/2}$ peak as a function of oxygen exposure for the quasicrystal surfaces. The peak shift as well as the FWHM gradually increases as exposure increases and almost saturates at around 100 L (note log scale in *x* axis). The chemical shift after 10^3 L of oxygen exposure is about 0.3 eV. This degree of chemical shift is expected if In_2O_3 is formed.[26] Figures 3(d) and 3(f) shows variations in the FWHM, position, and intensity of the $3d_{5/2}$ peak for the pure In foil. As in the quasicrystal, the FWHM shows a gradual increase with exposure. The peak grows asymmetrically at higher binding-energy side as exposure increases, resulting in an increase in the width. The FWHM remain almost same at higher exposure. This indicates that the oxidation begins at low exposure and saturates at certain exposure. We observed few differences between the quasicrystal and the pure foil. First, the energy shift in the pure foil seems to occur only after a certain coverage in contrast to a gradual increase in the quasicrystal. Second, the FWHM and energy shift at maximum exposure are slightly larger in the foil than in the quasicrystal. However, because of experimental uncertainly, we cannot confirm whether these differences are intrinsic.

The quantitative analysis of the Ag 3*d* levels for the quasicrystal surfaces is given in Figs. 3(g)–3(i). The FWHM and the position of the Ag 3*d* peaks remain unchanged for all exposures. We also studied the exposure of a Ag (111) surface to the same amount of oxygen and found no changes in the core-level peaks. This indicates that Ag in the quasicrystal is as inert as pure Ag for the given conditions. The sticking coefficient of the Ag (111) for oxygen at pressures and temperature employed is almost negligible.[31] It was previ-

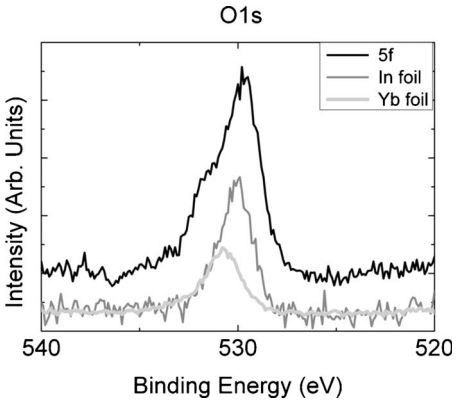

FIG. 4. O 1*s* spectra from the fivefold *i*-Ag-In-Yb surface (black), In foil (dark gray), and Yb foil (light gray) after oxygen exposure. Exposure was 10^3 L for the fivefold surface and In foil and 10 L for Yb foil.

ously found that the Ag (111) surface may be oxidized if the oxidation is carried out at temperature higher than room temperature[32] or if exposure is very high.[31]

Figure 2(d) shows the change in the O 1*s* level with oxygen exposure. At very low exposure, the O 1*s* spectra exhibit only one peak at 529.6 eV. Increasing exposure develops an additional peak at higher binding energy. By comparing these spectra with the O 1*s* spectra from the Yb and In foils after oxidation (Fig. 4), we ascribe the peak at 529.6 eV to oxide species of indium oxide and the other peak to oxide species of ytterbium oxide. The peak position at 529.6 eV is in good agreement with O 1*s* species of In_2O_3 reported previously.[26,33] Because of the overlap with the oxide peak of In, it is difficult to determine the precise position of the O 1*s* peak for ytterbium oxide from this spectrum. This is, however, possible after desorbing oxygen bound to In. Annealing the oxidized surface at 250 °C causes a desorption of oxygen bound to In, yielding a well-defined peak of ytterbium oxide (see below). The position of the peak is determined to be 530.8 eV, which is close to the value expected for Yb_2O_3.[29] The intensity of the O 1*s* peak is larger for indium oxide than ytterbium oxide as expected from the composition of the sample.

We now compare the oxidation behavior of the fivefold, threefold, and twofold surfaces. The variation in the FWHM and chemical shift of Ag 3*d*, In 3*d*, and Yb 4*d* with oxygen exposure is almost identical for all surfaces (Fig. 3). The variation in the O 1*s* intensity is also similar for the three surfaces. This, as well as the fact that experiments were carried out under the same oxygen pressure and substrate temperature, suggests that the sticking coefficient (intake of oxygen) is very similar for three orientations. The intensity of the In 3*d* peaks decreases faster for the fivefold surface than for the other two surfaces. This could be due to different roughness: if a surface is flat and oxygen is adsorbed atop, a uniform layer of oxide species would be formed. Photoelectrons would have to pass through the layer and thus intensity would decrease. At this point, we note that the threefold surface is difficult to clean, becoming contaminated by the residual gases in the UHV chamber within a few minutes following the preparation. The contamination was evidenced

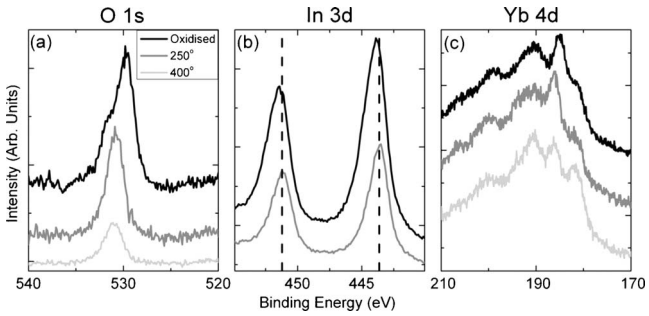

FIG. 5. (a) O 1*s*, (b) In 3*d*, and (c) Yb 4*d* spectra from the fivefold *i*-Ag-In-Yb surface after 10^3 L oxygen exposure and annealing at different temperatures (given in inset). The vertical dotted line marks the peak position for the clean surface.

by the change in the line shape of the Yb 4*d* level (not shown) and also in the valence-band structure studied using ultraviolet photoemission spectroscopy.[19] This indicates that the threefold surface is more active than other surfaces at early stage of oxidation.

Stability of the oxide layer

The stability of the oxide states was investigated by annealing the oxidized surface at different temperatures up to 400 °C, close to the temperature used for surface preparation. The annealing time for each temperature was about 15 min. Figure 5 shows the O 1*s*, In 3*d*, and Yb 4*d* peaks recorded after the sample is oxidized and subsequently annealed at 250 and 400 °C. The O 1*s* peak of indium oxide disappears at 250 °C, indicating that oxygen bound to In is desorbed at this temperature. Interestingly, the O 1*s* peak for ytterbium oxide increases in intensity when the O 1*s* peak of indium oxide disappears. This can be explained if oxygen bound to In transfers to Yb at this temperature. The desorption of oxygen from In sites is confirmed also by the change in the In 3*d* spectra. After annealing, the position and the FWHM of the In 3*d* level are identical to those obtained for the clean surface [Fig. 5(b)].

The O 1*s* peak of ytterbium oxide is still detectable after annealing at 400 °C, suggesting that oxygen is more strongly bound to Yb than In. This is expected from the heats of formation of bulk oxides which are −1815 kJ mol^{-1} for Yb_2O_3 and −926 kJ mol^{-1} for In_2O_3 at room temperature.[34] Since the heat of formation for Ag_2O is −31 kJ mol^{-1}, which is much less than that for ytterbium and indium oxides, Ag is expected to be inert.[34] This is consistent with our observations.

Thickness of the oxide layer

We performed polar angle-dependent XPS measurements in order to estimate the thickness of the oxide layer formed in UHV under the maximum exposure used of 10^3 L. Figure 6 shows the intensity of the O 1*s* ($I_{O\,1s}$) and Ag 3*d* ($I_{Ag\,3d}$) peaks as a function of polar angles (θ) taken from the fivefold surface. The intensity was calculated after normalizing the spectra for each angle with respect to the background intensity. The O 1*s* intensity increases and the Ag 3*d* inten-

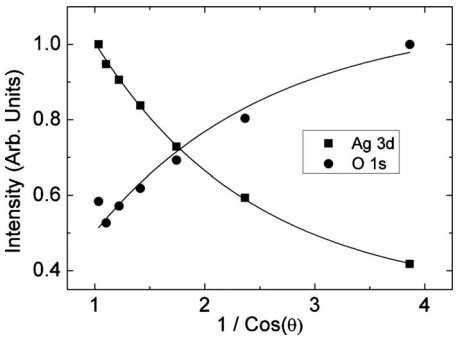

FIG. 6. XPS intensity of the O 1*s* and Ag 3*d* peaks as a function of polar angles (θ) taken from the fivefold *i*-Ag-In-Yb surface after 10^3 L oxygen exposure. The O 1*s* intensity is the total of indium oxide and ytterbium oxide. Solid curves are results of the fit with exponential functions (see text).

sity decreases exponentially with increasing grazing angles. The exponential decay of the Ag 3*d* intensity is expected from the Beer-Lambert formula: $I_{\mathrm{Ag}\ 3d} \propto e^{-d/\lambda_{\mathrm{Ag}\ 3d}\cos\theta}$, where $\lambda_{\mathrm{Ag}\ 3d}$ is the inelastic mean-free path of the Ag 3*d* photoelectrons and *d* is the thickness of the oxide layer, if a uniform oxide layer is formed. Similarly, increase in the O 1*s* intensity is expected to be $I_{\mathrm{O}\ 1s} \propto (1-e^{-d/\lambda_{\mathrm{O}\ 1s}\cos\theta})$. The observed intensity variation fits very well with the Beer-Lambert formula (see results of fit in Fig. 6). The thickness calculated from the fit is 1.1($\pm$0.10) nm. The value of λ used in the calculation was determined using the Tanuma-Powell-Penn equation[35] assuming that the photoelectrons travel through the layer of indium oxide and ytterbium oxide. The density of the oxide layer was calculated using the composition of Yb and In determined from XPS analysis discussed in Sec. III A. We cross checked the value of *d* determined as above by comparing the XPS intensity from the clean and oxidized surface at a given polar. For this, the intensity of the Ag 3*d* peaks from the clean surface ($I^{\circ}_{\mathrm{Ag}\ 3d}$) and from the oxidized surface ($I_{\mathrm{Ag}\ 3d}$) was measured for two different polar angles 15° and 45°. The value of *d* calculated again using the Beer-Lambert formula, $I_{\mathrm{Ag}\ 3d}=I^{\circ}_{\mathrm{Ag}\ 3d}e^{-d/\lambda_{\mathrm{Ag}\ 3d}\cos\theta}$ is 1.3($\pm$0.3) nm, which is close to the value obtained above.

Ordering of the oxide layer

We employed STM and LEED to study surface ordering after oxidation. Our experimental setup allowed us to measure STM images on the same area of the surface after different oxygen exposures. The tenfold Fourier transform of the clean surface STM images disappear soon after oxygen exposure starts (<1 L) suggesting that the oxidation destroys the quasicrystalline order in the surface. However, the step-terrace structure of the surface could be observed even after exposure 10^4 L, maximum employed exposure. The terraces were found to be very rough after oxidation. No LEED patterns could be observed from the surface after oxidation, revealing disorder oxide layer, consistent with STM results.

C. Oxidation in air and water

The O 1*s*, In 3*d*, and Yb 4*d* spectra from the fivefold *i*-Ag-In-Yb surface after air and water exposure are given in

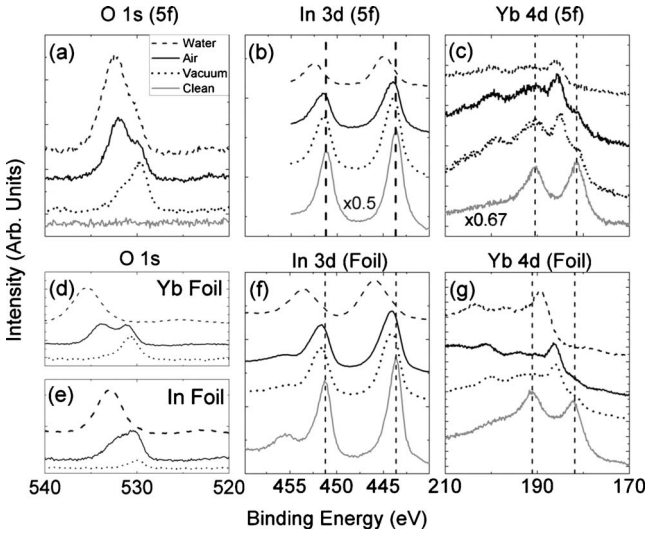

FIG. 7. O 1*s*, In 3*d*, and Yb 4*d* spectra from the clean surface (solid gray) and after exposure to oxygen in vacuum (dotted black), air (solid black), and water (dashed black) {[(a)–(c)]: fivefold *i*-Ag-In-Yb; [(d) and (g)]: Yb foil, and [(e) and (f)]: In foil}. The vertical dotted line marks the peak position for the clean surface.

Figs. 7(a)–7(c). The corresponding spectra from the clean surface and after in-vacuum oxidation are also presented in the same figure for comparison. The same core levels for the In and Yb foils are presented in Figs. 7(d)–7(g). The peak positions for each spectrum are compared in Table II. The Ag core levels remained unchanged after exposing to air and water, as in the case of in-vacuum oxidation. Therefore, these are not shown here.

TABLE II. Binding energies of the In 3*d* and O 1*s* core levels for the fivefold *i*-Ag-In-Yb surface, In foil and Yb foil after oxidation in vacuum, air, and water. The data for clean samples are also given. The values are in the units of electron volt. Uncertainty in the peak position is $\pm$(0.1–0.2) eV except the values marked by * which have a large degree of uncertainty because of the low intensity and the overlap with the other oxide peak.

		O 1*s* (oxide)		
	In $3d_{5/2}$	In	Yb	O 1*s* (hydroxide)
5f *i*-Ag-In-Yb				
Clean	443.6			
O_2 exposed	443.9	529.6	530.8	
Air exposed	444.0		*529.7	531.9
Water exposed	444.9		*530.0	532.4
In foil				
Clean	443.6			
O_2 exposed	444.0	530.2		
Air exposed	444.1	530.4		*532.6
Water exposed	445.9			533.0
Yb foil				
Clean				
O_2 exposed			530.7	
Air exposed			531.0	533.7

The In 3*d* peaks for the quasicrystal are identical in position and width when oxidized in vacuum and in atmosphere. Similarly, features observed in the Yb 4*d* spectra after air exposure are almost identical to those after in-vacuum oxidation, suggesting that the exposure of the sample to these two environments results in the same degree of oxidation. As shown in Fig. 7(f), the In foil also exhibits similar oxidation behavior in air and in oxygen in vacuum. The same is true for the Yb foil [Fig. 7(g)].

The O 1*s* spectra from the quasicrystal after air exposure still exhibit two peaks as after in-vacuum oxidation. However, the peak at higher binding energy is larger [Fig. 7(a)], in contrast to the result after in-vacuum oxidation where the peak at lower binding energy is dominant. The increase in intensity at higher binding energy is due to hydroxide species and physisorbed oxygen. This is expected because the sample is contaminated by hydroxide species in addition to oxygen, carbon, and other elements after exposing to air. The O 1*s* spectra from the In and Yb foils after air exposure also exhibit hydroxide species at higher binding energies [Figs. 7(d) and 7(e) consistent with the results from the quasicrystal.

After the quasicrystal was exposed to water, the Yb 4*d* peaks showed no remnant of metallic peaks whereas the metallic contribution was still detected after in-vacuum and air oxidation. This indicates that the oxidation of the quasicrystal is much more effective or complete in water than in-vacuum or air oxidation. The In 3*d* peaks are shifted to higher binding energies by an additional 1.3 eV. The shift is comparable (within experimental uncertainty) with that for pure In after water exposure,[26] which is due to the formation of hydroxide species. Here we note that the Ag core levels after water exposure remain same as of the clean surface. This confirms that there is no change in the position of the Fermi level after water exposure. As expected the O 1*s* spectra is also dominated by hydroxide species in the quasicrystal but also in the In foil [Fig. 7(e)] after water exposure. The Yb 4*d* and O 1*s* spectra from the Yb foil after water exposure are also shifted to higher binding energies (the O 1*s* peak is at 535.5 eV) but the shift is larger than expected. This is probably due to charging of the insulating oxide layer. The Yb foil was found to be highly corroded and discolored after water exposure.

IV. CONCLUSIONS

Employing XPS, we have characterized the core levels of the clean fivefold, threefold, and twofold surfaces of the *i*-Ag-In-Yb quasicrystal. Compared to pure elements, the core levels of Ag in the quasicrystal are shifted to higher binding energies and the Yb core levels to lower binding energies, whereas the In core are unchanged. This indicates a charge transfer from Ag to Yb in the quasicrystal alloy. The observed Yb core levels are the characteristic of divalent Yb.

We have also used XPS to study oxidation of these surfaces in three environments: vacuum, air, and water. The results are compared with those from the pure elements Ag, In, and Yb oxidized under the same conditions. Ytterbium is highly reactive, Ag is very inert and In shows moderate reactivity. This is expected from the heats of formation of the bulk oxide of the elements. Exposure to oxygen in vacuum and air results in the same degree of oxidation. However, the oxidation in water is more effective. STM and LEED results suggest that oxidation destroys the quasicrystalline order of the clean surface. To conclude, it is found that elements in the quasicrystal show oxidation behavior similar to that of the pure elements Ag, In, and Yb.

ACKNOWLEDGMENTS

This work was supported by Engineering and Physical Sciences Research Council (Grants No. EP/D071828/1 and No. EP/DO5253X/1). One of the authors (G.S.) is grateful for additional support from the EPSRC. We would like to thank J. A. Smerdon for a critical reading of the manuscript.

[1] D. Shechtman, I. Blech, D. Gratias, and J. W. Cahn, Phys. Rev. Lett. **53**, 1951 (1984).
[2] Z. M. Stadnik, in *Physical Properties of Quasicrystals*, edited by Z. M. Stadnik (Springer, Berlin, 1999).
[3] J.-M. Dubois, P. Brunet, W. Costin, and A. Merstallinger, J. Non-Cryst. Solids **334-335**, 475 (2004).
[4] J. Dolinšek, P. J. McGuiness, M. Klanjšek, I. Smiljanić, A. Smontara, E. S. Zijlstra, S. K. Bose, I. R. Fisher, M. J. Kramer, and P. C. Canfield, Phys. Rev. B **74**, 134201 (2006).
[5] D. Popović, D. Naumović, M. Bovet, C. Koitzsch, L. Schlapbach, and P. Aebi, Surf. Sci. **492**, 294 (2001).
[6] S.-L. Chang, J. W. Anderegg, and P. A. Thiel, J. Non-Cryst. Solids **195**, 95 (1996).
[7] P. A. Thiel, Prog. Surf. Sci. **75**, 69 (2004).
[8] A. P. Tsai, J. Q. Guo, E. Abe, H. Takakura, and T. J. Sato, Nature (London) **408**, 537 (2000).
[9] H. Takakura, C. P. Gomez, A. Yamamoto, M. de Boissieu, and A. P. Tsai, Nature Mater. **6**, 58 (2007).
[10] R. Tamura, T. Takeuchi, C. Aoki, S. Takeuchi, T. Kiss, T. Yokoya, and S. Shin, Phys. Rev. Lett. **92**, 146402 (2004).
[11] Y. Ishii and T. Fujiwara, Phys. Rev. Lett. **87**, 206408 (2001).
[12] A. L. Pope, T. M. Tritta, R. Gagnon, and J. Strom-Olsen, Appl. Phys. Lett. **79**, 2345 (2001).
[13] Y. Muro, T. Sasakawa, T. Sumemitsu, T. Takabatake, R. Tamurai, and S. Takeuchi, Jpn. J. Appl. Phys., Part 1 **41**, 3787 (2002).
[14] R. Tamura, Y. Murao, S. Takeuchi, K. Tokiwa, T. Watanabe, T. J. Sato, and A. P. Tsai, Jpn. J. Appl. Phys., Part 2 **40**, L912 (2001).
[15] C. Cui and A. P. Tsai, J. Cryst. Growth **312**, 131 (2010).
[16] H. R. Sharma, M. Shimoda, S. Ohhashi, and A. P. Tsai, Philos. Mag. **87**, 2989 (2007).
[17] H. R. Sharma, M. Shimoda, K. Sagisaka, H. Takakura, J. A. Smerdon, P. J. Nugent, R. McGrath, D. Fujita, S. Ohhashi, and A. P. Tsai, Phys. Rev. B **80**, 121401(R) (2009).
[18] H. R. Sharma, P. J. Nugent, J. A. Smerdon, M. Shimoda, S.

Ohhashi, C. Cui, J. L. V. Fournée, and A. P. Tsai, J. Phys.: Conf. Ser. **226**, 012004 (2010).
[19] H. R. Sharma, G. Simutis, V. R. Dhanak, P. J. Nugent, C. Cui, M. Shimoda, R. McGrath, A. P. Tsai, and Y. Ishii, Phys. Rev. B **81**, 104205 (2010).
[20] G. Trambly de Laissardière, D. Nguyen-Manh, and D. Mayou, Prog. Mater. Sci. **50**, 679 (2005).
[21] C. Cui, M. Shimoda, S. Ohhashi, and A. P. Tsai (unpublished).
[22] C. P. Goméz (private communication).
[23] S. Ohhashi, J. Hasegawa, S. Takeuchi, and A. P. Tsai, Philos. Mag. **87**, 3089 (2007).
[24] N. Fairley and A. Carrick, *The Casa Cookbook—Part 1: Recipes for XPS Data Processing* (Acolyte Science, UK, 2005).
[25] R. Hesse, T. Chassé, and R. Szargan, Fresenius' J. Anal. Chem. **365**, 48 (1999).
[26] C. Donley, D. Dunphy, D. Paine, C. Carter, K. Nebesny, P. Lee, D. Alloway, and N. R. Armstrong, Langmuir **18**, 450 (2002).
[27] J.-S. Chung, E.-J. Cho, and S.-J. Oh, Phys. Rev. B **41**, 5524 (1990).
[28] P. S. Bagus, F. Illas, G. Pacchioni, and F. Parmigiani, J. Electron Spectrosc. Relat. Phenom. **100**, 215 (1999).
[29] B. D. Padalia, W. C. Lang, P. R. Norris, L. M. Watson, and D. J. Fabian, Proc. R. Soc. London, Ser. A **354**, 269 (1977).
[30] V. Demange, J. W. Anderegg, J. Ghanbaja, F. Machizauda, D. J. Sordelet, M. Besser, P. A. Thiel, and J. M. Duboisa, Appl. Surf. Sci. **173**, 327 (2001).
[31] C. Benndorf, M. Franck, and F. Thieme, Surf. Sci. **128**, 417 (1983).
[32] A. I. Boronin, S. V. Koscheev, and G. M. Zhidomirov, J. Electron Spectrosc. Relat. Phenom. **96**, 43 (1998).
[33] R. W. Hewitt and N. Winograd, J. Appl. Phys. **51**, 2620 (1980).
[34] D. W. Wagman, W. H. Evans, V. B. Parker, R. H. Schumm, I. Halow, S. M. Bailey, K. L. Churney, and R. I. Nutall, J. Phys. Chem. Ref. Data **11**, 392 (1982).
[35] S. Tanuma, C. J. Powell, and D. R. Penn, Surf. Interface Anal. **17**, 911 (1991).